CRISPR activation screening identifies VGLL3-TEAD1-RUNX1/3 as a transcriptional complex for PD-L1 expression

Wijdeven, R.H.; Cabukusta, B.; Behr, F.M.; Qiu, X.; Amiri, D.; Borras, D.M.; ... ; Neefjes, J.

The Journal of Immunology

RESEARCH ARTICLE | SEPTEMBER 01 2022

CRISPR Activation Screening Identifies VGLL3–TEAD1–RUNX1/3 as a Transcriptional Complex for PD-L1 Expression

Ruud H. Wijdeven; ... et. al

J Immunol (2022) 209 (5): 907–915.
https://doi.org/10.4049/jimmunol.2100917

CRISPR Activation Screening Identifies VGLL3–TEAD1–RUNX1/3 as a Transcriptional Complex for PD-L1 Expression

Ruud H. Wijdeven,* Birol Cabukusta,* Felix M. Behr,† Xueer Qiu,‡ Deeba Amiri,‡ Daniel M. Borras,* Ramon Arens,† Yun Liang,‡ and Jacques Neefjes*

The PD-L1/2–PD-1 immune checkpoint is essential for the proper induction of peripheral tolerance and limits autoimmunity, whereas tumor cells exploit their expression to promote immune evasion. Many different cell types express PD-L1/2, either constitutively or upon stimulation, but the factors driving this expression are often poorly defined. In this study, using genome-wide CRISPR activation screening, we identified three factors that upregulate PD-L1 expression: GATA2, MBD6, and transcription cofactor vestigial-like protein 3 (VGLL3). VGLL3 acts as a transcriptional regulator, and its expression induced PD-L1 in many different cell types. Conversely, loss of VGLL3 impaired IFN-γ–induced PD-L1/2 expression in human keratinocytes. Mechanistically, by performing a second screen to identify proteins acting in concert with VGLL3, we found that VGLL3 forms a complex with TEAD1 and RUNX1/3 to drive expression of PD-L1/2. Collectively, our work identified a new transcriptional complex controlling PD-L1/2 expression and suggests that VGLL3, in addition to its known role in the expression of proinflammatory genes, can balance inflammation by upregulating the anti-inflammatory factors PD-L1 and PD-L2. ***The Journal of Immunology*****, 2022, 209: 907–915.**

The engagement of inhibitory checkpoint receptor PD-1 on $CD8^+$ T cells by its ligands PD-L1 and PD-L2 impairs T cell activation and effectively dampens the immune response (1, 2). Many different cell types express PD-L1 and, to a lesser extent, PD-L2, including tumor cells, immune cells, endothelial cells, and epithelial cells (3–5). Tumor cells express PD-L1 to promote immune evasion, and inhibition of the PD-1/PD-L1 checkpoint is now widely used in immunotherapy against many different tumor types (6, 7). However, immune cells and nonimmune cells, such as keratinocytes, express PD-L1 to induce peripheral tolerance, and the absence of PD-L1 on these cells leads to excessive immune activation and autoimmunity (2, 8–11).

Many cell types express PD-L1 constitutively at low levels, and this is boosted by proinflammatory stimuli, such as TLR activators and IFN-γ. Similar to many other immune genes, the PD-L1 promoter contains binding sites for AP-1, NF-κB, Myc, STAT, and IFN regulatory factor 1 (IRF1), the latter being responsible for IFN-γ–induced expression activation of PD-L1 (12–14). Tumor cell–specific expression of PD-L1 can be mediated via these transcription elements but also via copy number alterations, mRNA stabilization, or 3′ UTR shortening (15–18). Alternative mechanisms inducing PD-L1 expression include activation via YAP/TAZ, HIF1α, or ATF3 factors (19–22). However, these factors fail to explain the differential expression in all tumor cells. Furthermore, the mechanisms driving PD-L1 expression in specific subtypes of immune cells and nonimmune cells remain unknown. Recent genome-wide knockout screens for cell surface expression of PD-L1 have identified CMTM4 and CMTM6 as regulators of PD-L1 protein stability (23, 24), but no new transcriptional regulators.

To identify novel regulators of PD-L1 surface expression, we conducted a genome-wide CRISPR activation screen. This screen yielded a novel transcriptional regulator of PD-L1: transcription cofactor vestigial-like protein 3 (VGLL3). VGLL3 forms a complex with TEAD1 and RUNX1/RUNX3 to mediate PD-L1 expression and also functions in cooperation with IFN-γ. Furthermore, we show that VGLL3 is required for proper induction of PD-L1 and PD-L2 by IFN-γ in keratinocytes. Together, our work identifies new regulatory proteins controlling expression of the PD-L1 and PD-L2 immune checkpoint ligands.

Materials and Methods

Cell culture

MelJuSo cells were cultured in IMDM supplemented with 8% FCS, and cell line authentication was performed by Eurofins Genomics (19-ZE-000487). HEK 293T cells were obtained from the American Type Culture Collection (CRL-3216) and cultured in DMEM supplemented with 8% FCS. AKR, A375, FM3, SK-MEL-28, U87, U118, A549, BJeT, HaCaT, and retinal pigment epithelial cells were cultured in DMEM supplemented with 8% serum; DU145, PC3, H460, H1299, PC9, 5637, and BxPC3 cells were cultured in RPMI supplemented with 8% serum. Normal primary human keratinocytes were purchased from Lonza (Morristown, NJ) and cultured in Lonza KGM-gold keratinocyte growth medium according to the manufacturer's instructions. One day before cytokine stimulation, cells were switched to Lonza KBM medium to remove growth factors. Keratinocytes were used at passage 1 or 2.

Transfections, transductions, and Abs

For the generation of viral particles, HEK 293T cells were transfected using polyethyleneimine (Polysciences) with packaging plasmids pRSVrev, pHCMV-G VSV-G, and pMDLg/pRRE in combination with the lentiviral

*Department of Cell and Chemical Biology, Oncode Institute, Leiden University Medical Center, Leiden, the Netherlands; †Department of Immunology, Leiden University Medical Center, Leiden, the Netherlands; and ‡Department of Medical Microbiology & Immunology, University of Wisconsin–Madison, Madison, WI

ORCIDs: 0000-0002-3390-7384 (R.H.W.); 0000-0002-1187-3048 (B.C.); 0000-0002-1158-5011 (F.M.B.); 0000-0001-5058-4110 (R.A.); 0000-0001-6763-2211 (J.N.).

Received for publication September 21, 2021. Accepted for publication June 24, 2022.

This work was supported by Spinoza Premium and a European Research Council ERCOPE Advanced Grant (694307) awarded to J.N.

Address correspondence and reprint requests to Dr. Ruud H. Wijdeven or Jacques Neefjes, Department of Cell and Chemical Biology, Oncode Institute, Leiden University Medical Center, Einthovenweg 20, 2333 ZC Leiden, the Netherlands. E-mail addresses: r.h.m.wijdeven@lumc.nl (R.H.W.) or j.j.c.neefjes@lumc.nl (J.N.)

The online version of this article contains supplemental material.

Abbreviations used in this article: ChIP, chromatin immunoprecipitation; IRF1, IFN regulatory factor 1; MPH, MS2-p65-HSF1; qPCR, quantitative PCR; RSA, redundant siRNA activity; siRNA, small interfering RNA; T_N, naive $CD8^+$ T; Trq, turquoise; VGLL3, transcription cofactor vestigial-like protein 3.

construct. Virus was harvested and filtered, and target cells were transduced in the presence of 8 μg/ml polybrene (EMD Millipore). For coimmunoprecipitation experiments, HEK 293T cells were also transfected using polyethyleneimine.

For small interfering RNA (siRNA)-mediated depletion, cells were reverse transfected with Dharma FECT transfection reagent 1 and 50 nM siRNA (catalog numbers: siCtrl: D00120613-20, siTEAD1: M-012603-01-0005, siTEAD2: M-012611-00-0005, siTEAD3: M-012604-01-0005, siTEAD4: M-019570-03-0005) according to the manufacturer's protocol. Briefly, siRNAs and DharmaFECT were mixed and incubated for 20 min in a culture well, after which cells were added and left to adhere. Cells were analyzed 3 d after siRNA transfections. For gene depletion in keratinocytes, cells were electroporated using the Lonza 4D-Nucleofector following the manufacturer's recommendations.

Abs used in this study were as follows. For flow cytometry, we used PE anti-human CD274 (BioLegend), PE anti-human PD-L2 (BioLegend), and FITC anti-human HLA-ABC (BioLegend). For Western blotting, we used mouse anti–PD-L1 (Cell Signaling Technology, 29122), mouse anti-actin (Sigma-Aldrich, A5441), mouse anti-FLAG (Sigma-Aldrich, M2), rabbit anti-TEAD1 (ProSci, 22-472), mouse anti-TAZ (Santa Cruz Biotechnology, sc-518026), mouse anti-RUNX1 (Santa Cruz Biotechnology, sc-365644), mouse anti-RUNX3 (Santa Cruz Biotechnology, sc-101553), mouse anti-HA (Covance, 16B12), and rabbit anti-GFP and mouse anti-Myc (9E10) (for the latter two, as described in Ref. 25).

CRISPR activation and knockout screen

For CRISPR activation, the human CRISPR two-plasmid activation pooled library (SAM) was a gift from Feng Zhang (Addgene, 1000000078) and used for CRISPR activation screening. Stable MS2-p65-HSF1 (MPH)-expressing MelJuSo cells were generated, and 150 million MelJuSo MPH cells were infected at a multiplicity of infection of 0.3 with the SAM plasmid. The next day, cells were selected with hygromycin (200 μg/ml) and blasticidin (2.5 μg/ml), and, after 5 d, two batches of cells were stained for PD-L1, and the top 10% of PD-L1–expressing cells were sorted out using the FACS. Cells were grown out for another 6 d, and PD-L1^{high} cells were sorted again for both replicates. After the second sort, cells were grown out to reach 10 million, and genomic DNAs (gDNAs) were isolated and amplified using the established protocol (26). gRNAs were sequenced using the Illumina HighSeq 2500, and inserts were mapped to the reference. Statistical analysis was performed using redundant siRNA activity (RSA) analysis, and enrichment >4 was considered a hit (27).

For knockout screening, we used the human CRISPR Brunello genome-wide knockout library, a gift from David Root and John Doench (Addgene, 73178). MelJuSo cells stably expressing FLAG-VGLL3 were generated, and two batches of 100 million cells were infected at a multiplicity of infection of 0.3. Transduced cells were selected using puromycin (1 μg/ml), and, after 5 d, cells were stained for PD-L1, and the lowest 5% of GFP-positive PD-L1^{low}–expressing cells were sorted. Cells were grown out and sorted again using the same gating strategy as for the first sort. After this sort, cells were grown out to reach 10 million, the gDNA was isolated, and gDNAs were amplified using the established protocol (26). gRNAs were sequenced using the Illumina NovaSeq 6000, and inserts were mapped to the reference.

Hit validation and subcloning

For hit validation, two individual guides per gene were cloned into the LentiSAM vector (a gift from Feng Zhang, Addgene plasmid 75112), and MelJuSo MPH cells were stably transduced with these guides or with the empty LentiSAM as a control. Guide sequences used were as follows: GATA2-1: 5′-GGACTCCGGGACTGACCCGC-3′, GATA2-2: 5′-GTCCGCAATTCCCGA ACCGC-3′, MBD6-1: 5′-GGCTCCTGCGGCGGCGGCTG-3′, MBD6-2: 5′-TGCGCAGTGCCTTCTGGGAA-3′, VGLL3-1: 5′-GGGGAACGCCGGGGA GAAGG-3′, VGLL3-2: 5′-TGCCTCCCCAGGCTCTGACG-3′, ABCB5-1: 5′-CACATAACGTCTGTCTTGCC-3′, ABCB5-2: 5′-TCTAGTATCTAAGA AGACTG-3′, GPR173-1: 5′-AGTGGCATGAAGATGGGAGT-3′, GPR173-2: 5′-GTGTCCAACTAGCTGGCAGG-3′, SMARCC1-1: 5′- GATGCAGCC TACGGAGGATGG-3′, SMARCC1-2: 5′- GTCAAAAACCGGCGCTCAC TA-3′, TRIM54-1: 5′-ACCCATTCCTGAGTGAGTCA-3′, TRIM54-2: 5′-AC TCCCTTGAGCAAGGGCAG-3′.

For validation of the knockout screen, two individual guides per gene were cloned into the LentiCRISPR version 2 vector (a gift from Feng Zhang, Addgene plasmid 52961), and the indicated MelJuSo cells were transduced and selected using puromycin. Guide sequences were as follows: CD274: 5′-GGTTCCCAAGGACCTATATG-3′, TAZ-1: 5′-ATCCGAAGCCTAGCTCG TGG-3′, TAZ-2: 5′-ACGCGGGCGACGAGTGCGAG-3′, TEAD1-1: 5′-AC ATGGTGGATAGATAGCCA-3′, TEAD1-2: 5′-GGCCGGGAATGATTCA AACA-3′, RUNX1-1: 5′-CACTTCGACCGACAAACCTG-3′, RUNX1-2: 5′-TAGATGATCAGACCAAGCCC-3′, RUNX3-1: 5′-CCCCAGGATGCAT TATCCCG-3′, RUNX3-2: 5′-CACTGCGGCCCACGAAGCGA-3′, RUNX3-3: 5′-CCGTGCCGTACCTTGGATTG-3′.

Expression plasmids

Expression constructs for GATA2-FLAG (NM_001145661.2), FLAG-VGLL3 (NM_016206.4), FLAG-VGLL1, and GATA2Δ14 (NM_001145662) and VGLL3 mutants were made using Gateway cloning of the indicated genes into the pLenti-CAG-gate-FLAG-IRES-GFP vector, which was a gift from William Kaelin (Addgene plasmid 107398). For GATA2 (C373R), VGLL3 VHFAAA (V166A, H167A, F170A), and VGLL3 ΔHIS (Δ242-248), the mutagenesis primers as depicted in Table I were used. Turquoise (Trq)-RUNX1, Trq-TEAD1, Myc-VGLL3, and HA-RUNX1 were generated by subcloning these genes into the Trq-C1, 2Myc-C1, or 2HA-C1 vectors. All constructs were sequence verified.

Flow cytometry

Cells were trypsinized and stained for the indicated Abs in 2% FCS PBS for 30 min at 4°C. After washing, cells were analyzed on the BD LSR II, and data were analyzed using FlowJo software.

cDNA synthesis and quantitative PCR (qPCR)

RNA isolation (Bioline) and cDNA synthesis (Roche) were performed according to the manufacturer's instructions. SYBR Green (Bioline) signal was detected on the Bio-Rad analyzer and normalized to GAPDH using the Pfaffl formula. Primers used for detection of signals can be found in Table I. Actinomycin D was purchased from Santa Cruz Biotechnology.

Coimmunoprecipitation and Western blotting

For coimmunoprecipitation experiments, cells were lysed in lysis buffer (0.5% Nonidet P-40, 5% glycerol, 150 mM NaCl, 50 mM Tris-HCl, pH 8.0, 5 mM $MgCl_2$ supplemented with complete EDTA-free protease inhibitor cocktail [Roche]) and cleared by centrifugation. Lysates were incubated with Myc-Trap beads (Chromotek) or protein G-Sepharose 4 FF resin preloaded with the indicated Abs. Following incubations, beads were washed extensively with lysis buffer before addition of SDS sample buffer (2% SDS, 10% glycerol, 5%2-ME, 60 mM Tris-HCl, pH 6.8, and 0.01% bromophenol blue).

For whole-cell lysate analyses, cells were lysed directly in SDS sample buffer. Samples were boiled before loading, and proteins were separated by SDS-PAGE and transferred to Western blot filters. Blocking of the filter and Ab incubations were performed in PBS supplemented with 0.1% (v/v) Tween 20 and 5% (w/v) milk powder. Blots were imaged using the Odyssey Imaging System (LI-COR Biosciences) or the Amersham Imager. Full, uncropped Western blots are shown in Supplemental Fig. 4.

Chromatin immunoprecipitation (ChIP)-qPCR

For ChIP, the DNA of 5 million cells per primer pair was crosslinked using 1% paraformaldehyde; quenched with glycine; and washed with LB1, LB2, and LB3 as described in (28). Chromatin was fragmented using sonication and subjected to immunoprecipitation using a GFP Ab (Ctrl) or FLAG Ab overnight. After washing extensively, DNA was reverse crosslinked, isolated, and amplified using primers covering the PD-L1 promoter site from region −54 to +98: 5′-CAAACTGGATTTGCTGCCTTGG-3′ and 5′-CTACCTG CAGGCGGACAGAAG-3′. Data were normalized to input signal to obtain relative DNA occupancy.

T cell killing assays

Human PBMCs were obtained from buffy coats of healthy donors using Ficoll-Paque Plus (GE Healthcare) gradient centrifugation. Written informed consent for the use of these cells was obtained (Sanquin, Amsterdam, the Netherlands). $CD8^+$ T cells were enriched to a purity of ±90% using MACS with the CD8 T cell negative isolation kit (Miltenyi Biotec). Subsequently, naive $CD8^+$ T (T_N) cells were isolated by FACS for CCR7 and CD45RA on a CytoFLEX SRT cell sorter (Beckman Coulter) yielding $CCR7^+$ $CD45RA^+$ T_N cells. T cells were cultured in IMDM (Life Technologies) supplemented with 5% (v/v) pooled human serum (heat-inactivated; PAN Biotech), 100 U/ml penicillin, 100 μg/ml streptomycin, and 5 mM L-glutamine (Life Technologies) at 37°C and 5% CO_2.

T_N cells were activated for 48 h with αCD3 (clone 1XE, kindly provided by Ester Remmerswaal, Amsterdam UMC) and 1 μg/ml αCD28 (clone CD28.2, BioLegend). Cells were harvested and retrovirally transduced with the MART1 TCR (1D3), as previously described (29). The following day, cells were cultured for 3 d in the presence of 10 ng/ml rhIL-15 and rhIL-7 (PeproTech). Successfully transduced T cells were then identified using anti-mTCRβ (clone H57-597, BioLegend) and isolated by sorting on a CytoFLEX SRT cell sorter (Beckman Coulter) to obtain MART1 TCR^+ T cells. Sorted cells were cultured for another 8 d in the presence of 10 ng/ml rhIL-15 and rhIL-7 (PeproTech).

Table I. Primer sequences

Primer Name	Sequence 5′–3′
GATA2 C373R forward	5′-CCCTGTCTGCAACGCCCGTGGCCTCTAC-3′
GATA2 C373R reverse	5′-GCAGCTTGTAGTAGAGGCCACGGGCGTTGCAG-3′
VGLL3 VHFAAA forward	5′-GGGAGACATTGGGTCAGTAGCGGATGAAGCCGCCTCAAGAGCTTTGG-3′
VGLL3 VHFAAA reverse	5′-GGCTTGGCCCAAAGCTCTTGAGGCGGCTTCATCCGCTACTGACCC-3′
VGLL3 ΔHIS forward	5′-CCACCGCCCTCCTGCTGGCTCTGCCCTGG-3′
VGLL3 ΔHIS reverse	5′-CAGGAGGGCGGTGGCGGTGGTGCATGTGG-3′
GAPDH qPCR forward	5′-TGTTGCCATCAATGACCCCTT-3′
GAPDH qPCR reverse	5′-CTCCACGACGTACTCAGCG-3′
CD274 qPCR forward	5′-GGTGCCGACTACAAGCGAAT-3′
CD274 qPCR reverse	5′-AGCCCTCAGCCTGACATGTC-3′
PD-L2 qPCR forward	5′-GTCTTGGGAGCCAGGGTGAC-3′
PD-L2 qPCR reverse	5′-TGAAAGTGCAAATGGCAAGC-3′
Tead1 qPCR forward	5′-ATGGAAAGGATGAGTGACTCTGC-3′
Tead1 qPCR reverse	5′-TCCCACATGGTGGATAGATAGC-3′
Tead2 qPCR forward	5′-CTTCGTGGAACCGCCAGAT-3′
Tead2 qPCR reverse	5′-GGAGGCCACCCTTTTTCTCA-3′
Tead3 qPCR forward	5′-TGGACCCTCTCAGGACATCAA-3′
Tead3 qPCR reverse	5′-CCAGGGGCTCATAACTGCTG-3′
Tead4 qPCR forward	5′-GGACACTACTCTTACCGCATCC-3′
Tead4 qPCR reverse	5′-TCAAAGACATAGGCAATGCACA-3′

To induce PD1 expression on T cells, transduced T cells were activated with αCD3/αCD28 Dynabeads (Thermo Fisher Scientific) at a cell-to-bead ratio of 1:1 in the presence of 150 U/ml IL-2. Every 72 h, beads were magnetically removed, and the T cells were harvested and restimulated with a fresh batch of αCD3/αCD28 Dynabeads and IL-2. After three restimulations, T cells were harvested. Surface PD1 expression was confirmed by flow cytometric analysis, and the T cells were used in cytotoxicity assays.

To measure cytotoxicity, AKR and MelJuSo HLA-A2 YFP cells transduced with FLAG or FLAG-VGLL3 were plated in 96-well plates and cocultured with MART1 TCR$^+$ T cells at 0:1, 1:1, and 1:5 E:T ratios for 6 h. Dead cells were quantified by flow cytometry with the Zombie NIR viability kit (BioLegend) within GFP$^+$ target cells. To determine cytokine production by T cells, culture medium was supplemented with 5 μg/ml brefeldin A (BioLegend), and intracellular cytokine staining was performed after 6 h of coculture using the Cytofix/Cytoperm Kit (BD Biosciences) according to the manufacturer's recommendations.

Results

A CRISPR activation screen identifies GATA2, MBD6, and VGLL3 as regulators of PD-L1 expression

The immune checkpoint inhibitor PD-L1 is expressed in many tissues at varying levels, suggesting that several mechanisms are in play controlling its expression. To identify novel regulators promoting PD-L1 cell surface expression, MelJuSo cells were transduced with a genome-wide CRISPR/Cas9-mediated gene activation library targeting 23,000 genes of the human genome (26, 30) (Fig. 1A). This human cutaneous melanoma cell line expresses low levels of PD-L1, which provides a window for detecting increased expression. Following transduction with the activation library, cells with increased PD-L1 surface expression were sorted twice by FACS and analyzed for gRNA enrichment compared with the input (Fig. 1A). Hits were considered on the basis of two criteria: two or more gRNAs per gene showed fourfold enrichment in the sorted population in two independent sorts, and this enrichment had to be statistically significant according to RSA analysis (Fig. 1B and Supplemental Fig. 1A). Based on these criteria, several hits were identified, with the top one being CD274, the gene encoding PD-L1. To validate these results, cell lines stably expressing individual gRNAs were generated. Analysis of PD-L1 surface expression in these cells revealed that guides activating GATA2, MBD6, and VGLL3 upregulated PD-L1 expression (Fig. 1C). Meanwhile, these guides did not affect expression of another cell surface marker, MHC class I. Indeed, these gRNAs upregulated the expression of their respective target genes (Supplemental Fig. 1B), identifying the transcription factor GATA2, transcriptional coactivator VGLL3 and polycomb-binding protein MBD6 as regulators of PD-L1 cell surface expression in the melanoma cell line MelJuSo.

GATA2 and VGLL3 regulate PD-L1 transcription

Due to their defined functions as transcriptional regulators, we followed up on GATA2 and VGLL3. To confirm gRNA specificity and eliminate the possibility of off-target effects, PD-L1 expression was assessed after overexpressing GATA2 and VGLL3 by cDNA expression plasmids. Both FLAG-tagged GATA2 and VGLL3 robustly upregulated expression of PD-L1 at the cell surface, protein, and mRNA levels (Fig. 1D–G). Interestingly, IFN-γ stimulation of GATA2- and VGLL3-overexpressing cells further boosted their PD-L1 expression, suggesting that GATA2 and VGLL3 cooperate with IFN-γ in promoting PD-L1 expression (Fig. 1E–G). GATA2 and VGLL3 also upregulated the expression of the PD-L1 homolog PD-L2 (Fig. 1E). Increased PD-L1 mRNA could be the consequence of mRNA stabilization or increased transcription. To test for the first, cells were cultured with transcriptional inhibitor actinomycin D, showing that GATA2 or VGLL3 did not affect the half-life of PD-L1 mRNA (Supplemental Fig. 1C). Overall, our results demonstrate that GATA2 and VGLL3 promote transcription of PD-L1 and PD-L2. GATA2 regulating PD-L1 expression was recently shown in glioblastoma cells as well (31).

VGLL3 induces PD-L1 in multiple cell types and impairs T cell–mediated cytotoxicity

VGLL3 is a transcriptional activator that has recently been shown to drive expression of several proinflammatory genes and is reported to be involved in the induction of autoimmunity in women (32–34). Our data show that VGLL3 also promotes the expression of the anti-inflammatory genes PD-L1 and PD-L2. To test whether VGLL3 directly regulated PD-L1 transcription, we performed ChIP-qPCR experiments using anti-FLAG Abs and were able to detect FLAG-VGLL3 at the PD-L1 promoter site (Fig. 2A). To analyze the breadth of PD-L1 regulation, VGLL3 was introduced in a panel of different cell lines. Many but not all cell types induced PD-L1 upon VGLL3 expression, indicating that upregulation of VGLL3 can induce PD-L1 expression in multiple cell types (Fig. 2B). Increased PD-L1 expression renders cells less sensitive to T cell–mediated cytotoxicity, suggesting that VGLL3 could dampen T cell activation. To test this, MART1 TCR$^+$ T cells were used in a

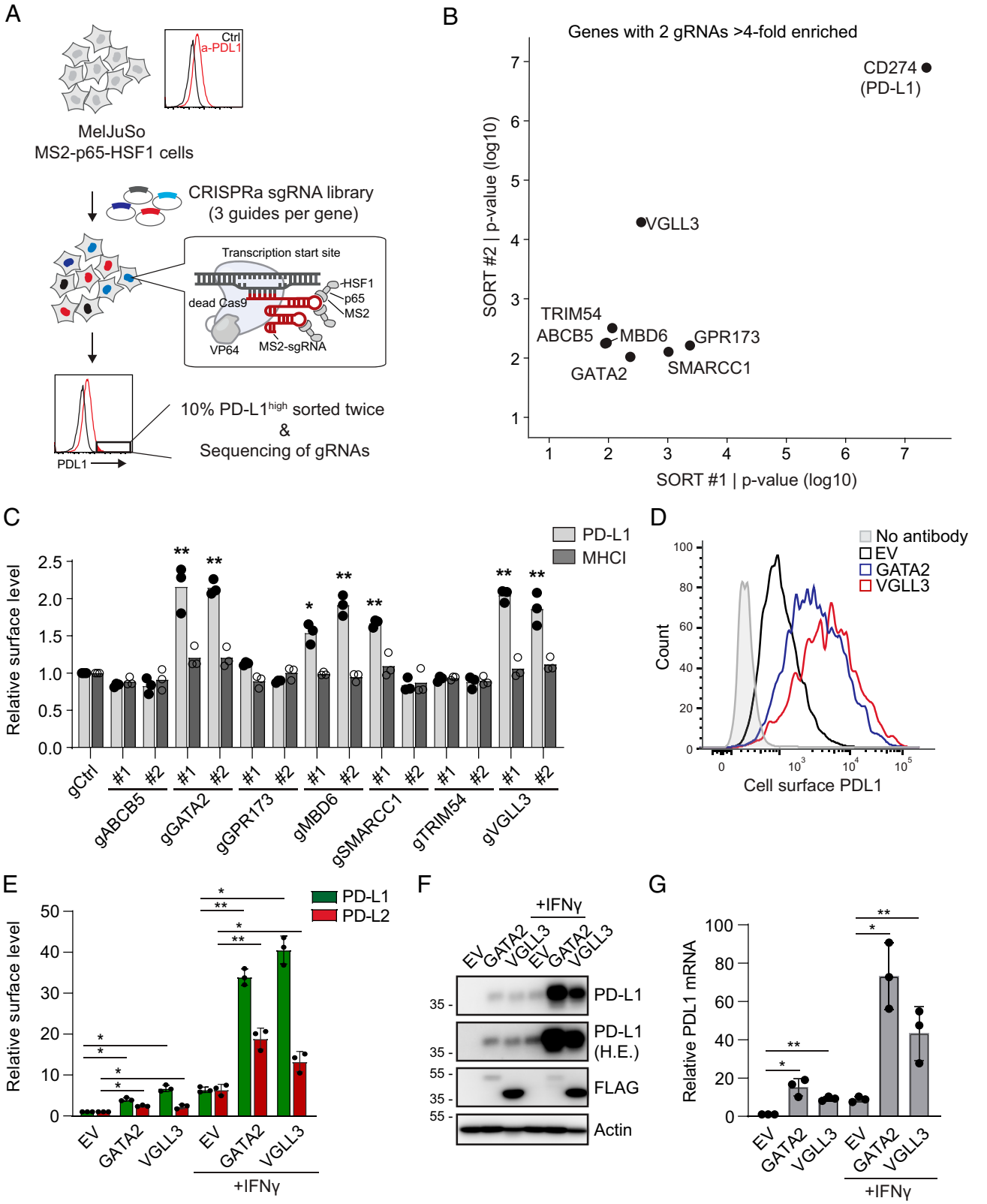

FIGURE 1. CRISPR activation screen identifies novel regulators of PD-L1 expression. (**A**) Schematic setup of the screen. MelJuSo melanoma cells stably expressing MS2-p65-HSF1 were transduced with a pooled gRNA library containing dCAS9 and sorted by FACS for cells displaying high levels of PD-L1. (**B**) Genes for which at least two different gRNAs were significantly enriched (greater than fourfold) in the sorted population versus control population in both replicate sorts. Plotted are *p* values based on RSA analysis. (**C**) MelJuSo MPH cells stably expressing the SAM vector with or without the indicated activation gRNAs were analyzed for cell surface expression of PD-L1 and MHC class I (HLA-ABC). Data represent three independent experiments (+SD), and statistical significance was determined by paired Student *t* test (*$p < 0.05$, **$p < 0.01$). (**D**) MelJuSo cells stably expressing FLAG (EV), GATA2-FLAG, or FLAG-VGLL3 were analyzed for cell surface expression of PD-L1 using flow cytometry. (**E**) MelJuSo cells as in D were either stimulated or not with IFN-γ for 48 h, and cell surface expression of PD-L1 and PD-L2 was measured using flow cytometry. (**F**) MelJuSo cells as in D were either stimulated or not with IFN-γ for 24 h, and expression of the indicated proteins was determined by Western blot analysis. (**G**) MelJuSo cells as in D were treated with IFN-γ for 24 h when indicated, and mRNA levels of the indicated genes were analyzed using quantitative real-time PCR and normalized to GAPDH. All data represent three independent experiments (+SD), and statistical significance was determined by ANOVA using Dunnett's multiple comparison test (*$p < 0.05$, **$p < 0.01$).

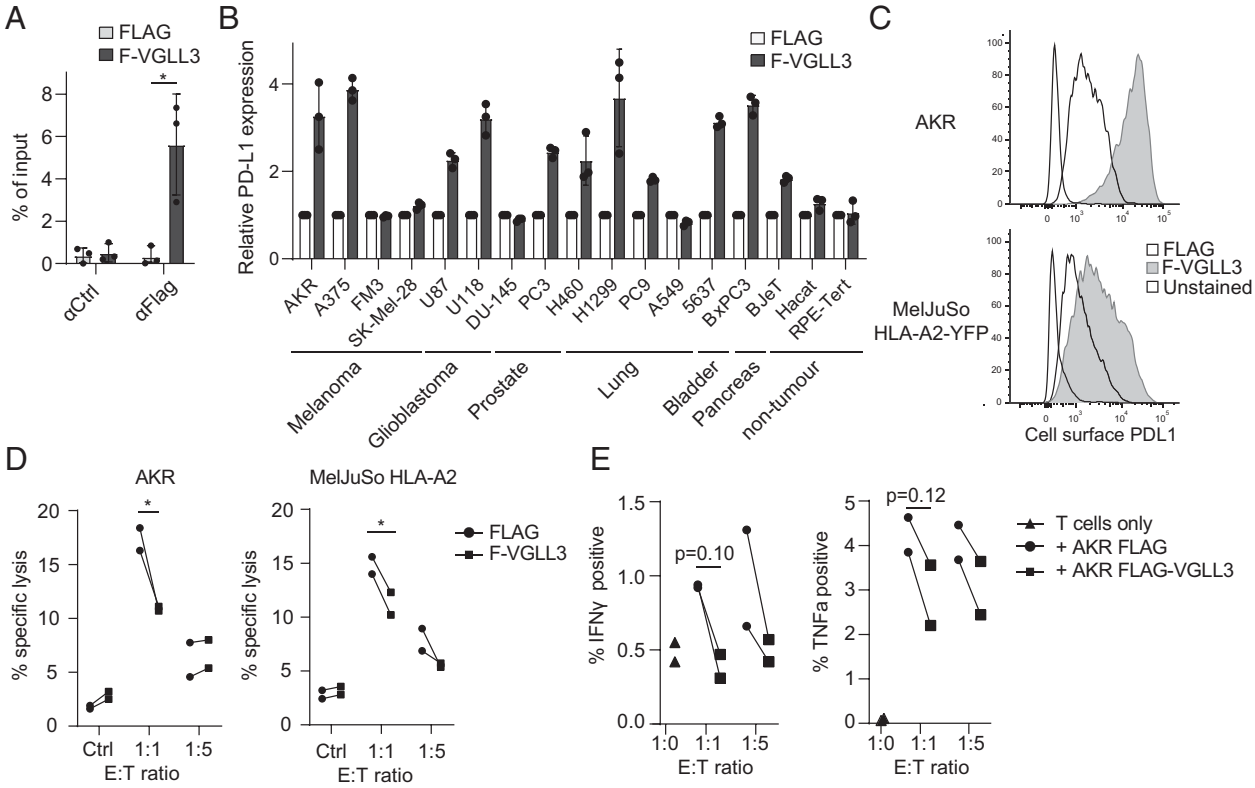

FIGURE 2. VGLL3 impairs T cell–mediated cytotoxicity. (**A**) ChIP-qPCR assay using either a control Ab (αGFP) or αFLAG Ab in MelJuSo cells expressing FLAG or FLAG-VGLL3. Isolated DNA for the PD-L1 promoter (−54 to +98 bp) was detected and quantified using qPCR and normalized to the input signal. Data represent three independent experiments (+SD). (**B**) Different cell lines were transduced with FLAG or FLAG-VGLL3 cDNA constructs. Four days later, cells were stained for PD-L1 and analyzed by flow cytometry. GFP^+ cells were gated, and PD-L1 expression was normalized to the FLAG-transduced cells. Tissue of origin of the cell types is provided below. $n = 3$ independent experiments. (**C**) AKR and MelJuSo HLA-A2-YFP cells were stably transduced with FLAG or FLAG-VGLL3 and analyzed for PD-L1 expression using flow cytometry. (**D**) AKR and MelJuSo HLA-A2-YFP cells from C were subjected to MART1 TCR^+ T cells at the indicated E:T ratio, and 6 h later, cells were stained using Zombie NIR cell labeling. GFP^+ tumor cells were gated, and the percentage of Zombie NIR positive cells was plotted. Ctrl represents tumor cells not exposed to T cells. Bars represent T cells from two independent donors. (**E**) T cells exposed or not to the indicated AKR cells as in D were stained intracellularly for IFN-γ and TNF-α and analyzed using flow cytometry. Cells positive for the indicated cytokine were quantified; data points represent T cells from two independent donors. For A, D, and E, statistical significance determined by ANOVA using Dunnett's multiple comparison test (*$p < 0.05$).

cytotoxicity experiment with target cells either expressing VGLL3 or not. As target cells, AKR ($HLA\text{-}A2^+MART1^+$) melanoma cells and MelJuSo cells ($MART1^+$) stably expressing HLA-A2-YFP were used. In both cases, PD-L1 expression was upregulated by VGLL3 (Fig. 2C). VGLL3 expression impaired killing of both cell types by T cells from two different donors in a manner correlating with the degree of PD-L1 upregulation (Fig. 2D). In agreement with this, T cells exposed to AKR cells expressing VGLL3 expressed less IFN-γ and TNF-α (Fig. 2E). Thus, VGLL3 can impair T cell–mediated killing.

VGLL3 regulates IFN-γ–induced PD-L1 and PD-L2 expression in keratinocytes

Physiologically, VGLL3 is highly expressed in keratinocytes (32), so we tested whether VGLL3 regulates PD-L1 and PD-L2 expression in keratinocytes. Indeed, mice overexpressing VGLL3 specifically in keratinocytes (under the keratin-5 promoter) expressed higher levels of PD-L1 and PD-L2 mRNA (33) (Fig. 3A). To validate that endogenous VGLL3 controls PD-L1/2 expression in these cells, primary keratinocytes were depleted for VGLL3 by RNAi, and expression of PD-L1 was assessed using Western blot and qPCR analyses. Although VGLL3 depletion did not significantly affect the basal levels of PD-L1/2 expression in these cells, IFN-γ–induced expression of PD-L1/2 was hampered when VGLL3 was depleted (Fig. 3B, 3C). Overall, these results show that VGLL3 is a physiological activator of IFN-γ–induced expression of PD-L1 and PD-L2 in keratinocytes.

VGLL3 controls PD-L1 transcription via TEAD1

Although VGLL3 upregulated PD-L1 in many cell types, the fact that not all cell types responded equally suggests that VGLL3 alone is not sufficient to promote PD-L1 expression. VGLL3 may then require additional (transcriptional) factors. To identify factors cooperating with VGLL3 in driving PD-L1 transcription, we performed a genome-wide CRISPR knockout screen in the MelJuSo FLAG-VGLL3–expressing cells, sorting for cells with reduced PD-L1 expression (Fig. 4A).

gRNA enrichment analysis of the sorted cells identified CD274 as the top hit, substantiating the screen (Fig. 4B). In addition to CD274, gRNAs targeting the NFs RUNX1, TAZ (WWTR1), and TEAD1 were significantly enriched (Supplemental Fig. 2A). It is reported that TAZ regulates PD-L1 expression in many tumor cells in conjunction with the TEAD transcription factors (21, 22). Moreover, VGLL3 interacts with TEAD transcription factors via its TDU domain to act as a transcriptional coactivator (35). This suggests that VGLL3 may interact with TEAD1 to drive PD-L1 expression in a manner similar to TAZ. To test this, we generated TAZ, TEAD1, and RUNX1 knockout cells using the top two gRNAs

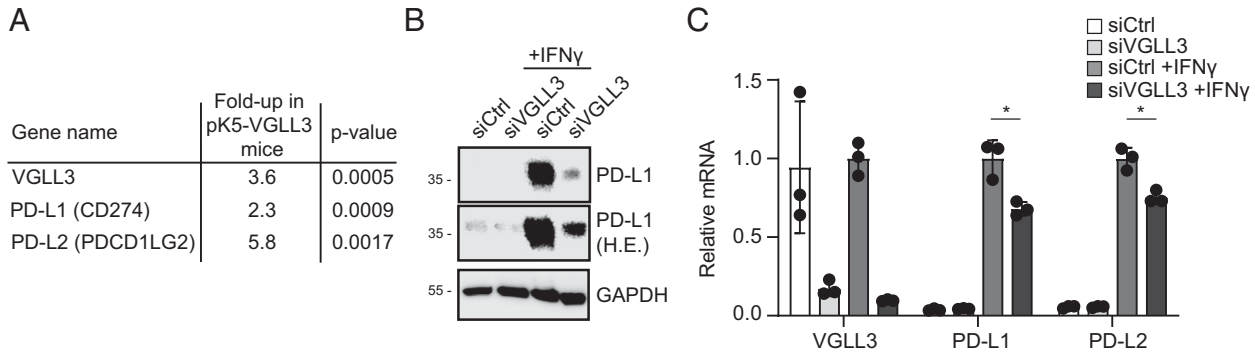

FIGURE 3. VGLL3 regulates IFN-γ–induced PD-L1 expression in keratinocytes. (**A**) Upregulation of VGLL3, PD-L1, and PD-L2 transcripts in the skin of mice overexpressing VGLL3 from the keratin 5 promoter. Data are from a transcriptome dataset (33). (**B**) Keratinocytes were transfected with siCtrl or siVGLL3 and treated or not with IFN-γ for 48 h, after which cells were lysed and PD-L1 expression was analyzed by Western blotting. $n = 2$. (**C**) Keratinocytes were transfected with siCtrl or siVGLL3, and mRNA for the indicated genes was analyzed from cells either treated or not with IFN-γ for 48h. Shown are data from three independent experiments (+SD); statistical significance was determined by ANOVA using Dunnett's multiple comparison test ($*p < 0.05$).

from the screen in both MelJuSo FLAG and MelJuSo FLAG-VGLL3 cells. gRNA-mediated knockout of TEAD1 in FLAG-VGLL3 cells almost completely abrogated VGLL3-mediated PD-L1 expression (Fig. 4C, 4D), whereas the effect on constitutive PD-L1 expression in MelJuSo cells was less prominent (Fig. 4D, right panel). However, the effect of TAZ knockout on PD-L1 surface expression was not affected by VGLL3 overexpression (Fig. 4D). This argues that TAZ is involved in canonical PD-L1 expression in MelJuSo cells and acts independently from VGLL3. Last, we found that the knockout of RUNX1 did not affect the existing PD-L1 expression but reduced VGLL3-mediated expression by ~50%.

To validate that the interaction between VGLL3 and TEAD1 is critical to drive PD-L1 expression, we generated a TDU domain mutant that in other VGLL family members abolishes TEAD binding (V166A, H167A, F170A). FLAG-tagged WT but not the vhfaaa-VGLL3 mutant was able to coimmunoprecipitate with MYC-tagged TEAD1 from transfected HEK293 cells, indicating that these mutations indeed abolished the interaction between VGLL3 and TEAD1. Indeed, the VGLL3(vhfaaa) mutant also failed to upregulate PD-L1 expression in MelJuSo cells (Fig. 4E). Of note, mutating a histidine stretch that is required for VGLL3 to control transcription in association with the ETS1 transcription factors did not show any effect on VGLL3-controlled PD-L1 expression (Supplemental Fig. 2B) (36). In line with these observations, RNAi-mediated depletion of specifically TEAD1 decreased VGLL3-dependent upregulation of PD-L1. Of the other TEAD proteins, only silencing of TEAD4 had a minor effect on VGLL3-induced PD-L1 expression, despite its being very highly expressed in these cells (Fig. 4F, 4G, and Supplemental Fig. 2C). Thus, VGLL3 interacts primarily with TEAD1 to drive PD-L1 expression. Introduction of VGLL1 into MelJuSo cells did not upregulate PD-L1, so the ability to upregulate PD-L1 is not conserved in the VGLL family but rather is restricted to VGLL3 (Supplemental Fig. 2D).

VGLL3 interacts with RUNX1 and RUNX3 to drive PD-L1 expression

Our knockout screen also identified RUNX1 as a candidate involved in VGLL3-mediated PD-L1 expression. To test whether VGLL3 interacts with RUNX1, VGLL3 was immunoprecipitated from lysates. RUNX1 coprecipitated with VGLL3, and the absence of TAZ and TEAD1 expression did not affect this interaction (Fig. 5A), suggesting that VGLL3 interacts with RUNX1 independently of TEAD1. In agreement with this, TDU-mutant VGLL3 interacted as strongly as wild-type VGLL3 with MYC-RUNX1 (Fig. 5B, 5C). Thus, TEAD1, RUNX1, and VGLL3 form a tripartite complex to drive PD-L1 expression. However, although TEAD1 was essential for VGLL3-driven PD-L1 expression, RUNX1 depletion only affected this partly. RUNX1 is homologous to and shares redundancy with RUNX3 (37), and both are expressed in MelJuSo cells. Therefore, we tested whether codepletion of RUNX1 and RUNX3 would render cells insensitive to VGLL3-induced PD-L1 expression. Double-knockout clones were generated using RUNX1 sgRNA 1 in combination with three different RUNX3 CRISPR knockout constructs. Each of these clones independently inhibited upregulation of PD-L1 expression after VGLL3 expression (Fig. 5D). Reintroduction of RUNX1 using a Trq-RUNX1 construct restored the ability of these cells to upregulate PD-L1 as analyzed by flow cytometry and Western blotting (Fig. 5E, 5F), indicating that RUNX1 and RUNX3 act redundantly in conjunction with VGLL3. Collectively, we propose that VGLL3 forms a transcriptional complex with TEAD1 and RUNX1/RUNX3 in control of PD-L1 expression.

Discussion

The PD-L1/2–PD-1 immune checkpoint is essential for the induction of peripheral tolerance and limiting autoimmunity, whereas tumor cells exploit it to promote immune evasion. Given the wide variety of cell types expressing PD-L1 and the major differences in expression levels, it is likely that many factors are involved in the control of PD-L1/2 expression. Several factors that independently drive PD-L1 transcription have been identified, but research has focused mostly on the pathways relevant in tumor cells. In this study, we used an unbiased CRISPR activation screen to identify novel factors regulating PD-L1. By doing so, factors usually not expressed in the model cell line can be identified, although it is limited to factors that can drive expression independently or in the genetic context of the selected cell line. In addition to the recently published transcription factor GATA2, we identified MBD6 and VGLL3 as novel regulators of PD-L1 expression. Whereas MBD6, a polycomb-interacting protein, was not further studied, VGLL3 was shown to complex with TEAD1 and RUNX1/3 to regulate PD-L1 transcription.

Although cytokine-induced PD-L1 expression and tumor cell expression of PD-L1 have been studied in detail, it is unknown which factors drive constitutive expression in different immune cell subsets and other cell types such as endothelial cells and keratinocytes. Our data, in combination with a study by Fu et al. (31), show that GATA2 facilitates PD-L1 expression. GATA2 is predominantly expressed in various immune cell types, as well as endothelial cells,

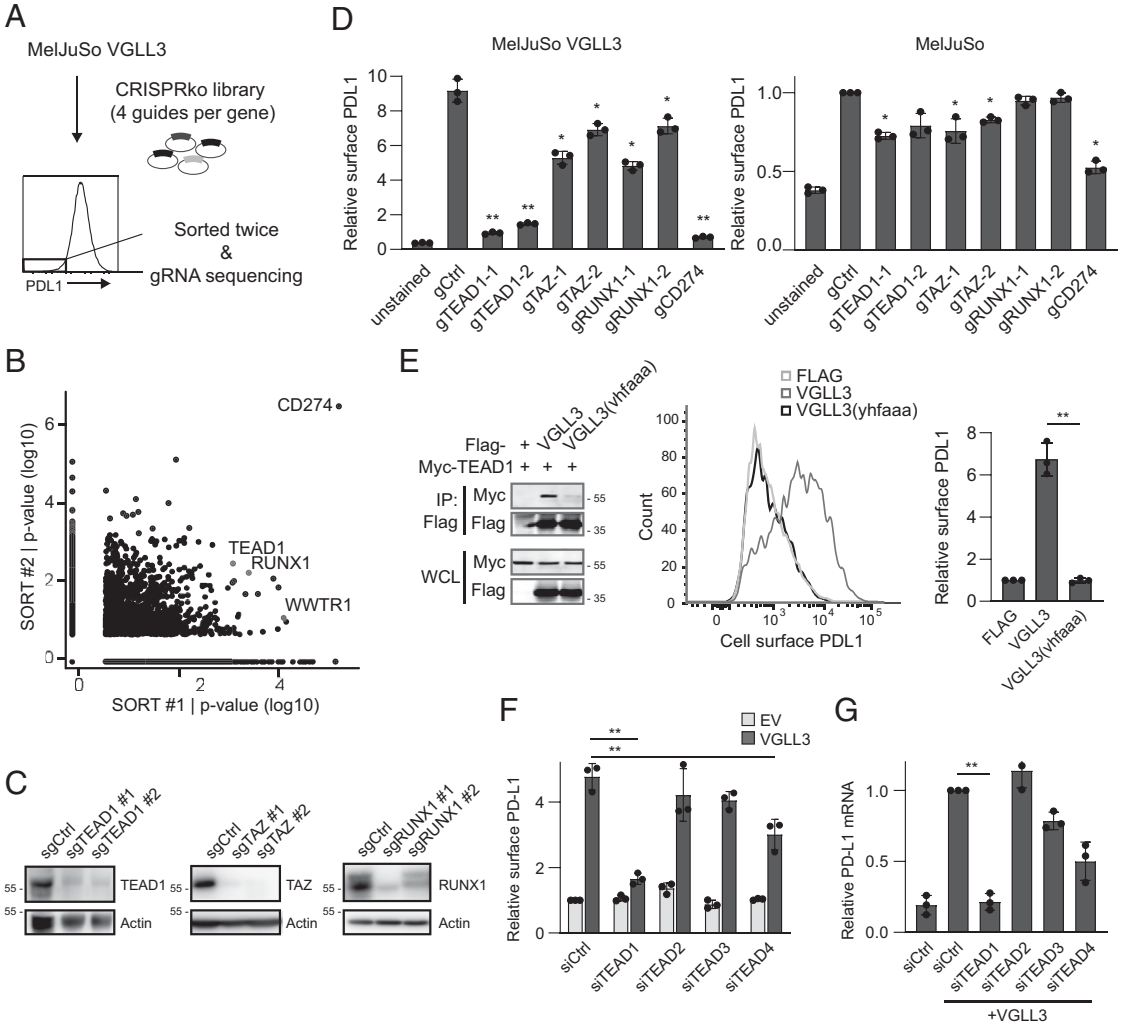

FIGURE 4. VGLL3 cooperates with TEAD1 to drive PD-L1 expression. (**A**) Schematic setup of the screen. MelJuSo cells stably expressing FLAG-VGLL3 were transduced with the Brunello CRISPR knockout library and sorted by FACS twice for cells displaying low PD-L1 surface levels. (**B**) Results of the RSA analysis of the inserts from the biological duplicates, with three candidates indicated with gray dots. (**C**) Western blot validation of the knockout efficiency of the pooled MelJuSo VGLL3 knockout cells transduced with the indicated gRNAs. (**D**) MelJuSo FLAG-VGLL3– or FLAG-expressing cells were transduced with the indicated gRNAs, and pooled knockout lines were analyzed for surface PD-L1 expression using flow cytometry. (**E**) Left: Myc or Myc-TEAD1 were isolated from HEK293T cells using Myc-TRAP beads, and associated FLAG-VGLL3 or FLAG-VGLL3(vhfaaa) was detected by Western blot analysis. Right: MelJuSo cells transduced with the indicated expression constructs were analyzed for expression of PD-L1 using flow cytometry. (**F**) MelJuSo cells stably expressing FLAG or FLAG-VGLL3 were transfected with the indicated siRNAs and 3 d later were analyzed for PD-L1 expression using flow cytometry. (**G**) As in F, but 3 d after siRNA transfection. mRNA was isolated, and the expression of PD-L1 transcript was analyzed by qRT-PCR and normalized to GAPDH mRNA. All data represent three independent experiments (+SD); statistical significance was determined by ANOVA using Dunnett's multiple comparison test ($*p < 0.05$, $**p < 0.01$).

which both have significant PD-L1 expression. Furthermore, GATA2 is highly expressed in hematopoietic stem cells, such as PD-L1/2, and their expression correlates during the different phases of stem cell development (38). It will be interesting to test whether GATA2 is indeed responsible for PD-L1/2 expression during hematopoiesis and what the physiological function is for this expression.

We also identified VGLL3 as a novel regulator of both PD-L1 and PD-L2 expression. VGLL3 is a transcriptional coactivator that can induce transcription via the TEAD transcription factors, as well as ETS1 (35, 36). We define a tripartite transcription complex consisting of VGLL3, TEAD1, and RUNX1/3 in the control of PD-L1 expression. The TEAD transcription factors contain four members, and although in our system TEAD1 appears to be dominant, it could be that in different cell types other TEAD family members act in concert with VGLL3. Similarly, RUNX1 and RUNX3 are very homologous and act redundantly to afford PD-L1 induction. The prerequisite for RUNX1/3 sets VGLL3 apart from YAP/TAZ, which also drive PD-L1 expression via the TEAD family and bind to the PD-L1 promoter (21, 22, 39, 40). However, RUNX1 and RUNX3 also interact with these factors, suggesting that VGLL3 and TAZ potentially act mechanistically similarly to drive PD-L1 expression. VGLL1, however, did not induce PD-L1 expression, and VGLL4 has been reported to induce PD-L1 independently from its interaction with the TEADs (41). This suggests that within the VGLL family, VGLL3 has specifically evolved to regulate PD-L1. The strong cooperation of IFN-γ with VGLL3 argues that IRF1 and VGLL3 act together at the PD-L1 promoter site. In line with this, IRF1-binding sites are adjacent to a TEAD-binding site (14, 21), together increasing potential for transcription.

VGLL3 is a transcriptional activator that displays a female-dominant expression and is linked to several autoimmune diseases that are more prevalent in women (32). It regulates the expression of many

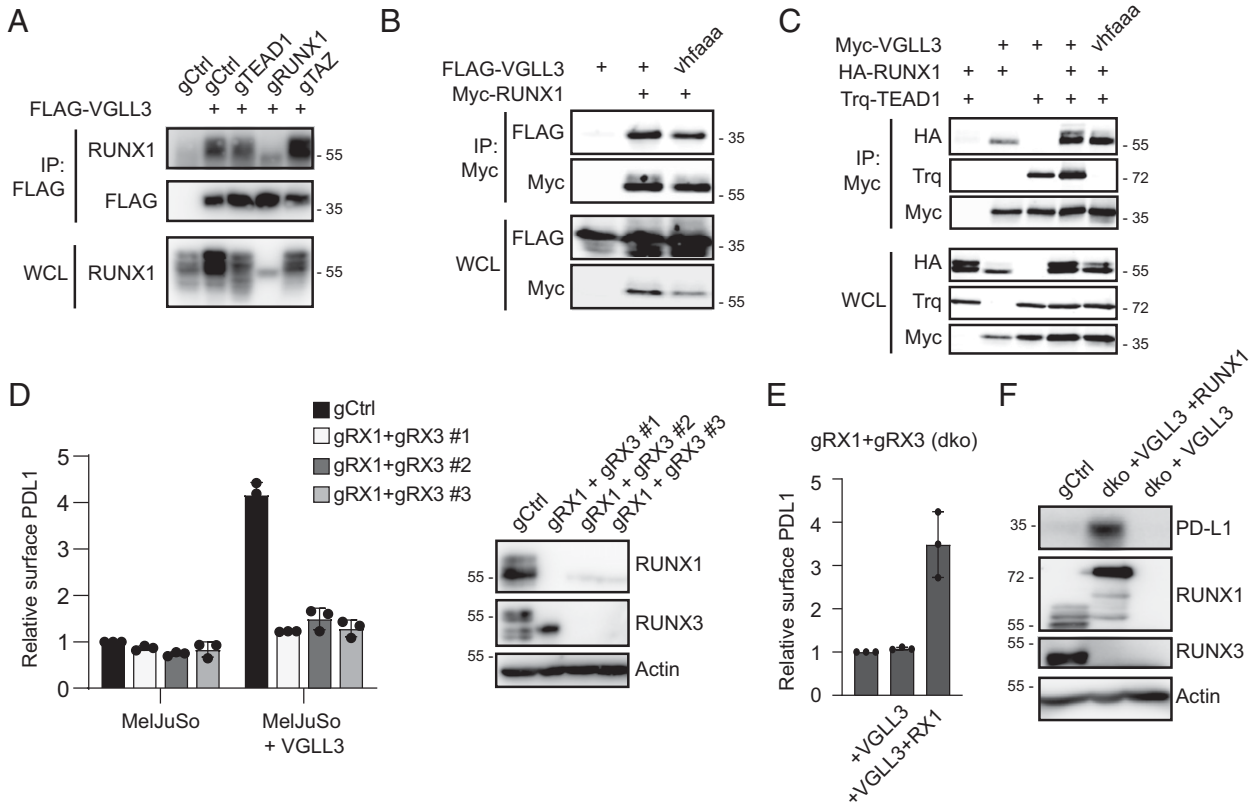

FIGURE 5. VGLL3 interacts with RUNX1/3 to drive PD-L1 expression. (**A**) MelJuSo cells with the indicated genetic background were lysed, and FLAG or FLAG-VGLL3 was immunoprecipitated. Associated RUNX1 was detected by Western blot analysis. (**B**) Myc or Myc-RUNX1 was isolated from HEK293T cell lysates using Myc-TRAP beads, and associated FLAG-VGLL3 or FLAG-VGLL3-vhfaaa mutant was detected by Western blot analysis. (**C**) Myc or Myc-VGLL3 was isolated from HEK 293T cell lysates using Myc-TRAP beads, and associated HA-RUNX1 or Trq-TEAD1 was detected by Western blot analysis. (**D**) MelJuSo cells or single-cell knockout clones of MelJuSo cells transduced with RUNX1 and RUNX3 targeting sgRNAs were either transduced or not with FLAG-VGLL3, and PD-L1 surface expression was analyzed by flow cytometry. (**E**) MelJuSo cells depleted for RUNX1 and RUNX3 were transfected with FLAG-VGLL3 and Trq-RUNX1 when indicated, and cell surface expression of PD-L1 was analyzed by flow cytometry. (**F**) MelJuSo cells either depleted or not for RUNX1 and RUNX3 (double knockout [dko]) were transduced with FLAG-VGLL3 and Trq-RUNX1 when indicated, and the indicated proteins were detected by Western blot analysis.

autoimmune-associated proinflammatory genes, and overexpression in keratinocytes leads to the development of a lupus-like rash and systemic autoimmunity, classified by enhanced B cell reactivity (32–34). Our data demonstrate that complementary to promoting expression of proinflammatory genes, VGLL3 induces expression of the anti-inflammatory factors PD-L1 and PD-L2, leading to evasion of T cell–mediated killing. Using the same models as before, mice expressing VGLL3 in keratinocytes were found to upregulate PD-L1/2, and keratinocytes were shown to require VGLL3 for full induction of PD-L1/PD-L2 by IFN-γ. Thus, VGLL3 promotes expression of genes from both sides of the pro- and anti-inflammatory equation. This resembles IFN-γ, which also promotes proinflammatory cytokines such as CXCL9 and CXCL10, as well as anti-inflammatory factors such as PD-L1 and PD-L2. However, expression of VGLL3 is limited to specific tissues. VGLL3 is not expressed in immune cells, which express high levels of PD-L1/2, but rather has its highest expression in trophoblasts, especially extravillous trophoblasts and syncytiotrophoblasts (Supplemental Fig. 3) (42, 43), which form the outer layer and protrusions of the placenta. These are also among the highest PD-L1– and PD-L2–expressing cells and secrete proinflammatory factors to recruit and shape an immune cell repertoire that maximally protects the fetus (44). We propose that these tissues use VGLL3 to create a well-balanced but active immune environment.

In summary, using a genome-wide CRISPR activation screen in combination with a dedicated genome-wide CRISPR knockout screen, we identified novel regulators of PD-L1 expression, including GATA2 and MBD6. VGLL3, a female-biased transcriptional activator linked to autoimmune disease, in complex with TEAD1 and RUNX1/3 can regulate transcription of PD-L1 and PD-L2. VGLL3 is required for full induction of PD-L1/2 expression by IFN-γ in keratinocytes and thus regulates not only expression of proinflammatory genes but also expression of the anti-inflammatory immune checkpoint molecules PD-L1 and PD-L2.

Acknowledgments

We thank the Leiden University Medical Center Flow Cytometry Facility for support and cell sorting and members of the Neefjes group for critical discussions.

Disclosures

The authors have no financial conflicts of interest.

References

1. Ishida, Y., Y. Agata, K. Shibahara, and T. Honjo. 1992. Induced expression of PD-1, a novel member of the immunoglobulin gene superfamily, upon programmed cell death. *EMBO J.* 11: 3887–3895.
2. Latchman, Y. E., S. C. Liang, Y. Wu, T. Chernova, R. A. Sobel, M. Klemm, V. K. Kuchroo, G. J. Freeman, and A. H. Sharpe. 2004. PD-L1-deficient mice show that PD-L1 on T cells, antigen-presenting cells, and host tissues negatively regulates T cells. *Proc. Natl. Acad. Sci. USA* 101: 10691–10696.

3. Ingram, J. R., M. Dougan, M. Rashidian, M. Knoll, E. J. Keliher, S. Garrett, S. Garforth, O. S. Blomberg, C. Espinosa, A. Bhan, et al. 2017. PD-L1 is an activation-independent marker of brown adipocytes. *Nat. Commun.* 8: 647.
4. Eppihimer, M. J., J. Gunn, G. J. Freeman, E. A. Greenfield, T. Chernova, J. Erickson, and J. P. Leonard. 2002. Expression and regulation of the PD-L1 immunoinhibitory molecule on microvascular endothelial cells. *Microcirculation* 9: 133–145.
5. Dong, H., S. E. Strome, D. R. Salomao, H. Tamura, F. Hirano, D. B. Flies, P. C. Roche, J. Lu, G. Zhu, K. Tamada, et al. 2002. Tumor-associated B7-H1 promotes T-cell apoptosis: a potential mechanism of immune evasion. *Nat. Med.* 8: 793–800.
6. Parsa, A. T., J. S. Waldron, A. Panner, C. A. Crane, I. F. Parney, J. J. Barry, K. E. Cachola, J. C. Murray, T. Tihan, M. C. Jensen, et al. 2007. Loss of tumor suppressor PTEN function increases B7-H1 expression and immunoresistance in glioma. *Nat. Med.* 13: 84–88.
7. Borghaei, H., L. Paz-Ares, L. Horn, D. R. Spigel, M. Steins, N. E. Ready, L. Q. Chow, E. E. Vokes, E. Felip, E. Holgado, et al. 2015. Nivolumab versus docetaxel in advanced nonsquamous non-small-cell lung cancer. *N. Engl. J. Med.* 373: 1627–1639.
8. Tewalt, E. F., J. N. Cohen, S. J. Rouhani, C. J. Guidi, H. Qiao, S. P. Fahl, M. R. Conaway, T. P. Bender, K. S. Tung, A. T. Vella, et al. 2012. Lymphatic endothelial cells induce tolerance via PD-L1 and lack of costimulation leading to high-level PD-1 expression on CD8 T cells. *Blood* 120: 4772–4782.
9. Keir, M. E., S. C. Liang, I. Guleria, Y. E. Latchman, A. Qipo, L. A. Albacker, M. Koulmanda, G. J. Freeman, M. H. Sayegh, and A. H. Sharpe. 2006. Tissue expression of PD-L1 mediates peripheral T cell tolerance. *J. Exp. Med.* 203: 883–895.
10. Nishimura, H., M. Nose, H. Hiai, N. Minato, and T. Honjo. 1999. Development of lupus-like autoimmune diseases by disruption of the PD-1 gene encoding an ITIM motif-carrying immunoreceptor. *Immunity* 11: 141–151.
11. Okiyama, N., and S. I. Katz. 2014. Programmed cell death 1 (PD-1) regulates the effector function of CD8 T cells via PD-L1 expressed on target keratinocytes. *J. Autoimmun.* 53: 1–9.
12. Zerdes, I., A. Matikas, J. Bergh, G. Z. Rassidakis, and T. Foukakis. 2018. Genetic, transcriptional and post-translational regulation of the programmed death protein ligand 1 in cancer: biology and clinical correlations. *Oncogene* 37: 4639–4661.
13. Casey, S. C., L. Tong, Y. Li, R. Do, S. Walz, K. N. Fitzgerald, A. M. Gouw, V. Baylot, I. Gütgemann, M. Eilers, and D. W. Felsher. 2016. MYC regulates the antitumor immune response through CD47 and PD-L1. *Science* 352: 227–231.
14. Garcia-Diaz, A., D. S. Shin, B. H. Moreno, J. Saco, H. Escuin-Ordinas, G. A. Rodriguez, J. M. Zaretsky, L. Sun, W. Hugo, X. Wang, et al. 2017. Interferon receptor signaling pathways regulating PD-L1 and PD-L2 expression. [Published erratum appears in 2019 *Cell Rep.* 29: 3766.] *Cell Rep.* 19: 1189–1201.
15. Kataoka, K., Y. Shiraishi, Y. Takeda, S. Sakata, M. Matsumoto, S. Nagano, T. Maeda, Y. Nagata, A. Kitanaka, S. Mizuno, et al. 2016. Aberrant PD-L1 expression through 3′-UTR disruption in multiple cancers. *Nature* 534: 402–406.
16. Coelho, M. A., S. de Carné Trécesson, S. Rana, D. Zecchin, C. Moore, M. Molina-Arcas, P. East, B. Spencer-Dene, E. Nye, K. Barnouin, et al. 2017. Oncogenic RAS signaling promotes tumor immunoresistance by stabilizing PD-L1 mRNA. *Immunity* 47: 1083–1099.e6.
17. Xu, Y., M. Poggio, H. Y. Jin, Z. Shi, C. M. Forester, Y. Wang, C. R. Stumpf, L. Xue, E. Devericks, L. So, et al. 2019. Translation control of the immune checkpoint in cancer and its therapeutic targeting. *Nat. Med.* 25: 301–311.
18. Inoue, Y., K. Yoshimura, K. Mori, N. Kurabe, T. Kahyo, H. Mori, A. Kawase, M. Tanahashi, H. Ogawa, N. Inui, et al. 2016. Clinical significance of PD-L1 and PD-L2 copy number gains in non-small-cell lung cancer. *Oncotarget* 7: 32113–32128.
19. Noman, M. Z., G. Desantis, B. Janji, M. Hasmim, S. Karray, P. Dessen, V. Bronte, and S. Chouaib. 2014. PD-L1 is a novel direct target of HIF-1α, and its blockade under hypoxia enhanced MDSC-mediated T cell activation. *J. Exp. Med.* 211: 781–790.
20. Liu, H., X. Kuang, Y. Zhang, Y. Ye, J. Li, L. Liang, Z. Xie, L. Weng, J. Guo, H. Li, et al. 2020. ADORA1 inhibition promotes tumor immune evasion by regulating the ATF3-PD-L1 axis. *Cancer Cell* 37: 324–339.e8.
21. Janse van Rensburg, H. J., T. Azad, M. Ling, Y. Hao, B. Snetsinger, P. Khanal, L. M. Minassian, C. H. Graham, M. J. Rauh, and X. Yang. 2018. The Hippo pathway component TAZ promotes immune evasion in human cancer through PD-L1. *Cancer Res.* 78: 1457–1470.
22. Feng, J., H. Yang, Y. Zhang, H. Wei, Z. Zhu, B. Zhu, M. Yang, W. Cao, L. Wang, and Z. Wu. 2017. Tumor cell-derived lactate induces TAZ-dependent upregulation of PD-L1 through GPR81 in human lung cancer cells. *Oncogene* 36: 5829–5839.
23. Mezzadra, R., C. Sun, L. T. Jae, R. Gomez-Eerland, E. de Vries, W. Wu, M. E. W. Logtenberg, M. Slagter, E. A. Rozeman, I. Hofland, et al. 2017. Identification of CMTM6 and CMTM4 as PD-L1 protein regulators. *Nature* 549: 106–110.
24. Burr, M. L., C. E. Sparbier, Y. C. Chan, J. C. Williamson, K. Woods, P. A. Beavis, E. Y. N. Lam, M. A. Henderson, C. C. Bell, S. Stolzenburg, et al. 2017. CMTM6 maintains the expression of PD-L1 and regulates anti-tumour immunity. *Nature* 549: 101–105.
25. Rocha, N., C. Kuijl, R. van der Kant, L. Janssen, D. Houben, H. Janssen, W. Zwart, and J. Neefjes. 2009. Cholesterol sensor ORP1L contacts the ER protein VAP to control Rab7-RILP-p150 Glued and late endosome positioning. *J. Cell Biol.* 185: 1209–1225.
26. Joung, J., S. Konermann, J. S. Gootenberg, O. O. Abudayyeh, R. J. Platt, M. D. Brigham, N. E. Sanjana, and F. Zhang. 2017. Genome-scale CRISPR-Cas9 knockout and transcriptional activation screening. [Published erratum appears in 2019 *Nat. Protoc.* 14: 2259.] *Nat. Protoc.* 12: 828–863.
27. König, R., C. Y. Chiang, B. P. Tu, S. F. Yan, P. D. DeJesus, A. Romero, T. Bergauer, A. Orth, U. Krueger, Y. Zhou, and S. K. Chanda. 2007. A probability-based approach for the analysis of large-scale RNAi screens. *Nat. Methods* 4: 847–849.
28. Schmidt, D., M. D. Wilson, C. Spyrou, G. D. Brown, J. Hadfield, and D. T. Odom. 2009. ChIP-seq: using high-throughput sequencing to discover protein-DNA interactions. *Methods* 48: 240–248.
29. Gomez-Eerland, R., B. Nuijen, B. Heemskerk, N. van Rooij, J. H. van den Berg, J. H. Beijnen, W. Uckert, P. Kvistborg, T. N. Schumacher, J. B. Haanen, and A. Jorritsma. 2014. Manufacture of gene-modified human T-cells with a memory stem/central memory phenotype. *Hum. Gene Ther. Methods* 25: 277–287.
30. Konermann, S., M. D. Brigham, A. E. Trevino, J. Joung, O. O. Abudayyeh, C. Barcena, P. D. Hsu, N. Habib, J. S. Gootenberg, H. Nishimasu, et al. 2015. Genome-scale transcriptional activation by an engineered CRISPR-Cas9 complex. *Nature* 517: 583–588.
31. Fu, Y., C. J. Liu, D. K. Kobayashi, T. M. Johanns, J. A. Bowman-Kirigin, M. O. Schaettler, D. D. Mao, D. Bender, D. G. Kelley, R. Uppaluri, et al. 2020. GATA2 regulates constitutive PD-L1 and PD-L2 expression in brain tumors. *Sci. Rep.* 10: 9027.
32. Liang, Y., L. C. Tsoi, X. Xing, M. A. Beamer, W. R. Swindell, M. K. Sarkar, C. C. Berthier, P. E. Stuart, P. W. Harms, R. P. Nair, et al. 2017. A gene network regulated by the transcription factor VGLL3 as a promoter of sex-biased autoimmune diseases. *Nat. Immunol.* 18: 152–160.
33. Billi, A. C., M. Gharaee-Kermani, J. Fullmer, L. C. Tsoi, B. D. Hill, D. Gruszka, J. Ludwig, X. Xing, S. Estadt, S. J. Wolf, et al. 2019. The female-biased factor VGLL3 drives cutaneous and systemic autoimmunity. *JCI Insight* 4: e127291.
34. Pagenkopf, A., and Y. Liang. 2020. Immunometabolic function of the transcription cofactor VGLL3 provides an evolutionary rationale for sexual dimorphism in autoimmunity. *FEBS Lett.* 594: 3371–3383.
35. Figeac, N., A. D. Mohamed, C. Sun, M. Schönfelder, D. Matallanas, A. Garcia-Munoz, E. Missiaglia, E. Collie-Duguid, V. De Mello, A. V. Pobbati, et al. 2019. VGLL3 operates via TEAD1, TEAD3 and TEAD4 to influence myogenesis in skeletal muscle. *J. Cell Sci.* 132: jcs225946.
36. Simon, E., N. Thézé, S. Fédou, P. Thiébaud, and C. Faucheux. 2017. Vestigial-like 3 is a novel Ets1 interacting partner and regulates trigeminal nerve formation and cranial neural crest migration. *Biol. Open* 6: 1528–1540.
37. Mevel, R., J. E. Draper, M. Lie-A-Ling, V. Kouskoff, and G. Lacaud. 2019. RUNX transcription factors: orchestrators of development. *Development* 146: dev148296.
38. Tober, J., M. M. W. Maijenburg, Y. Li, L. Gao, B. K. Hadland, P. Gao, K. Minoura, I. D. Bernstein, K. Tan, and N. A. Speck. 2018. Maturation of hematopoietic stem cells from prehematopoietic stem cells is accompanied by up-regulation of PD-L1. *J. Exp. Med.* 215: 645–659.
39. Miao, J., P.-C. Hsu, Y.-L. Yang, Z. Xu, Y. Dai, Y. Wang, G. Chan, Z. Huang, B. Hu, H. Li, et al. 2017. YAP regulates PD-L1 expression in human NSCLC cells. *Oncotarget* 8: 114576–114587.
40. Kim, M. H., C. G. Kim, S. K. Kim, S. J. Shin, E. A. Choe, S. H. Park, E. C. Shin, and J. Kim. 2018. YAP-induced PD-L1 expression drives immune evasion in BRAFi-resistant melanoma. *Cancer Immunol. Res.* 6: 255–266.
41. Wu, A., Q. Wu, Y. Deng, Y. Liu, J. Lu, L. Liu, X. Li, C. Liao, B. Zhao, and H. Song. 2019. Loss of VGLL4 suppresses tumor PD-L1 expression and immune evasion. *EMBO J.* 38: e99506.
42. Vento-Tormo, R., M. Efremova, R. A. Botting, M. Y. Turco, M. Vento-Tormo, K. B. Meyer, J. E. Park, E. Stephenson, K. Polański, A. Goncalves, et al. 2018. Single-cell reconstruction of the early maternal-fetal interface in humans. *Nature* 563: 347–353.
43. Veras, E., R. J. Kurman, T. L. Wang, and I. M. Shih. 2017. PD-L1 expression in human placentas and gestational trophoblastic diseases. *Int. J. Gynecol. Pathol.* 36: 146–153.
44. Mor, G., P. Aldo, and A. B. Alvero. 2017. The unique immunological and microbial aspects of pregnancy. *Nat. Rev. Immunol.* 17: 469–482.